



feature



Building on the success of osimertinib: achieving CNS exposure in oncology drug discovery

Nicola Colclough¹, nicola.colclough@astrazeneca.com, Kan Chen², Peter Johnström³, Markus Fridén^{4,5} and Dermot F. McGinnity¹

Due to the blood–brain barrier (BBB) limiting the exposure of therapeutics to the central nervous system (CNS), patients with brain malignancies are challenging to treat, typically have poor prognoses, and represent a significant unmet medical need. Preclinical data report osimertinib to have significant BBB penetration and emerging clinical data demonstrate encouraging activity against CNS malignancies. Here, we discuss the oncology drug candidates AZD3759 and AZD1390 as case examples of discovery projects designing in BBB penetrance. We demonstrate how these innovative kinase inhibitors were recognized as brain penetrant and outline our view of experimental approaches and strategies that can facilitate the discovery of new brain-penetrant therapies for the treatment of primary and secondary CNS malignancies as well as other CNS disorders.

Introduction

Brain metastases are the most commonly observed intracranial tumors. Approximately 40–50% of patients with non-small cell lung cancer (NSCLC) will develop brain metastases during the course of their disease [1,2]. Primary brain tumors include glioblastoma (GBM), with an incidence of 2–3 per 100 000 adults per year [3]. These patient groups are difficult to treat, have a poor prognosis (GBM median survival is 12–15 months [4,5], brain metastases median survival is 3–6 months [6]), and represent a clinically significant unmet need.

The BBB limits the exposure of compounds to the brain and is thought to be a primary reason for the lack of efficacy of therapeutic agents in these patients [7]. The BBB comprises endothelial cells with tight junctions (TJs), and drug

transport into the brain must be via either passive transcellular diffusion or active uptake. The endothelial cells of the BBB contain multiple efflux transporters, of which P-glycoprotein (P-gp) [encoded by multidrug resistance gene 1 (MDR1)] and breast cancer resistance protein (BCRP) are the most important and actively pump compounds from the brain into the blood [8]. Both belong to the ATP-binding cassette family of transporters (MDR1/ABCB1; BCRP/ABCG2). P-gp in particular demonstrates broad substrate specificity [9].

Brain tumors can cause disruption of the BBB, such that it becomes 'leaky' [10,11]. It is frequently debated whether this offers a possible route for drug delivery while sparing healthy brain tissue. However, to date, clinical studies

have been relatively inconclusive in terms of demonstrating significant CNS efficacy by this route (e.g., lapatinib, gefitinib, and erlotinib) [7]. Indeed, micrometastatic sites and the small tumor cells at the leading edge of a GBM, which are not visible on MRI, may be protected by the healthy BBB [12,13]. As such, it is seen as desirable for a new generation of oncology drugs targeting primary or secondary CNS tumors to have good BBB penetrant properties and to be able to readily distribute into the brain across a healthy intact BBB.

While recognising the importance of good BBB penetrance properties in oncology drugs aimed at treating brain tumors and metastases, the data used to assess and claim BBB penetrance can often be limited, with preclinical data

tending to focus predominantly on distribution of total levels of drug (total brain/total plasma ratio; Kp) in rodents [14,15]. To achieve a full picture of BBB penetrance, a comprehensive and complementary set of preclinical assays is required, incorporating the assessment of human and animal transporter substrate liability, free brain:free plasma ratios (K_{puu}) and brain imaging studies in rodents and nonrodents. Such assays, models, and approaches have been incorporated into a comprehensive CNS strategy at AstraZeneca (AZ), validated with marketed CNS small-molecule drugs and successfully utilized in the BBB penetrance assessment and/or design of osimertinib, AZD3759, and AZD1390.

Osimertinib

Osimertinib is a potent, orally bioavailable, and selective irreversible epidermal growth factor receptor tyrosine kinase inhibitor (EGFR-TKI) of both activating and T790M resistance mutations [16,17]. It is a recommended first-line treatment option for patients with EGFR mutation (EGFR_m) advanced NSCLC, and for patients with T790M positive NSCLC, following disease progression on first or second generation EGFR-TKIs. In the FLAURA clinical trial, NSCLC patients with brain metastases showed a reduced risk of CNS progression or death (52%) when taking osimertinib as first line treatment compared with patients taking gefitinib or erlotinib [18,19]. CNS progression-free survival was also improved in NSCLC patients taking osimertinib compared with standard platinum chemotherapy in the second-line setting (11.7 months versus 5.6 months, respectively) [20]. Gefitinib, erlotinib, and chemotherapy are all drugs considered to have poor BBB permeability [21–23]. Osimertinib has shown activity in patients with EGFR_m NSCLC with leptomeningeal metastases (LM), a rarer CNS metastasis with particularly devastating prognosis (32 patients; ten showed radiological improvement and 13 showed stable disease, with a median treatment duration of 6 months at a 160 mg dose) [24].

Many NSCLC patients with progressive disease will have brain metastases and so the ability of osimertinib to cross the BBB giving sufficient brain exposure to drive antitumor efficacy is desired. As such, osimertinib has been evaluated using a range of preclinical BBB *in vitro*, *in vivo*, and imaging assays [21]. Nonhuman primates represent the closest *in vivo* model for predicting human brain exposure, expressing similar levels of P-gp and BCRP in the BBB to humans (within twofold) and sharing 93–97% amino acid sequence homology for the P-gp transporter [25,26]. As such, PET imaging

studies in macaques are particularly informative [27]. Figure 1a reveals that osimertinib achieves significant brain penetrance with a brain/blood Kp = 2.6 and fast distribution into the brain following intravenous (IV) dosing, plateauing at 1.29% (± 0.42 ; N = 3) of injected radioactivity at 10 min (%ID) [21]. In the macaque, a %ID value of ~1% indicates a compound that distributes equally across the body based on average monkey brain weight (60 mg [28]) relative to bodyweight (5.9–7.0 kg in this study). This supports the observed encouraging clinical data in the CNS setting. (Note macaque brain K_{puu} was not determined as the contribution to Kp from irreversible covalent binding of [¹¹C]osimertinib to brain and blood tissue could not be readily calculated.)

Designing oncology compounds with brain exposure

In oncology projects that aim to develop compounds to treat primary or secondary tumors of the brain, good brain exposure is key. Compounds should readily permeate the healthy BBB and give rise to free brain levels that, ideally, are equivalent to, or greater than, free levels in plasma (i.e., K_{puu} ≥ 1). This minimizes the need for dose escalation to achieve CNS efficacy, which can result in toxicity because of higher systemic exposure. In practical terms, it is necessary to have a K_{puu} value that delivers unbound drug levels at the target site in the brain for the necessary duration to drive clinical efficacy. As such, preclinical pharmacokinetics (PK)/pharmacodynamics (PD)/efficacy studies in brain metastases models are useful to establish these relationships [21,29,30]. The most important consideration in achieving the goal of good BBB penetrance for oral 'drug-like' small-molecule therapies is the design of compounds that are not substrates of the human efflux transporters [31]. Consequently, sensitive *in vitro* transporter assays expressing the most important BBB human efflux transporters (P-gp and BCRP) are important to have as a first-line assay as part of compound design (Fig. 2).

It is important to stress that when designing brain-penetrant drugs the assays in the BBB cascade (Fig. 2) are used in parallel with the usual collection of drug discovery assays to design potent and selective candidate drugs with acceptable PK and drug–drug interaction profiles. As such, adding the additional design hurdle of reducing transporter substrate activity to an existing generic oral drug target profile can be challenging to achieve in practice. Moreover, predictive *in silico* approaches, plus simple, robust *in vitro* assays with enhanced

throughput capacity, are an absolute requirement to maximize the opportunity to design in CNS-penetrance properties.

In silico BBB

Physicochemical properties typically used to describe optimal CNS drug space include molecular size, hydrogen bond-donating ability, polarity, ionization state (pKa), and lipophilicity (logD/P) [32]. Numerous quantitative–structure activity (QSAR) models have been built utilizing these and other descriptors to predict likely brain exposure. Within AZ, a QSAR model trained on rat brain K_{puu} values has been established [33,34]. This model emphasizes the importance of hydrogen bonding in contrast to lipophilicity, which was not a determinant of unbound brain exposure [33].

Key in the design of BBB-penetrant compounds is the ability to design out efflux transporter substrate liability. QSAR models that accurately predict efflux liability have proved challenging to establish, reflecting the broad specificity of transporters, such as P-gp. At AZ, a global QSAR model trained on in-house *in vitro* P-gp efflux assay data has been developed, providing a useful input to project design strategies. A global model is also available for predicting apparent intrinsic permeability (Papp) trained on in-house Caco-2 cell monolayer data including efflux transporter inhibitors [35]. This model is helpful in confirming that molecules are not hindered by poor passive diffusion through the cells of the BBB, although for projects focused on brain-penetrant oral 'drug-like' small molecules, this is not frequently an issue.

In vitro human efflux transporter assessment

In vitro cell culture monolayers, such as those formed from Madin–Darby canine kidney (MDCK) cells overexpressing the human efflux transporters P-gp and BCRP, provide a useful model for the BBB. As in the BBB, the cells in these assays form TJs. The efflux ratio of compounds in these MDCK assays can be readily determined by measuring the apparent permeability (Papp) in the B to A direction across the monolayer and dividing by the measured permeability in the A to B direction. The efflux ratio enables classification of compounds as transporter substrates and also provides an initial estimate of the affinity of the compound for the transporter (assuming permeability of the compound at both the membranes is symmetric).

Typically, MDCK assays use cells singly transfected with human efflux transporters (e.g., MDCK_MDR1 or MDCK_BCRP). However, more

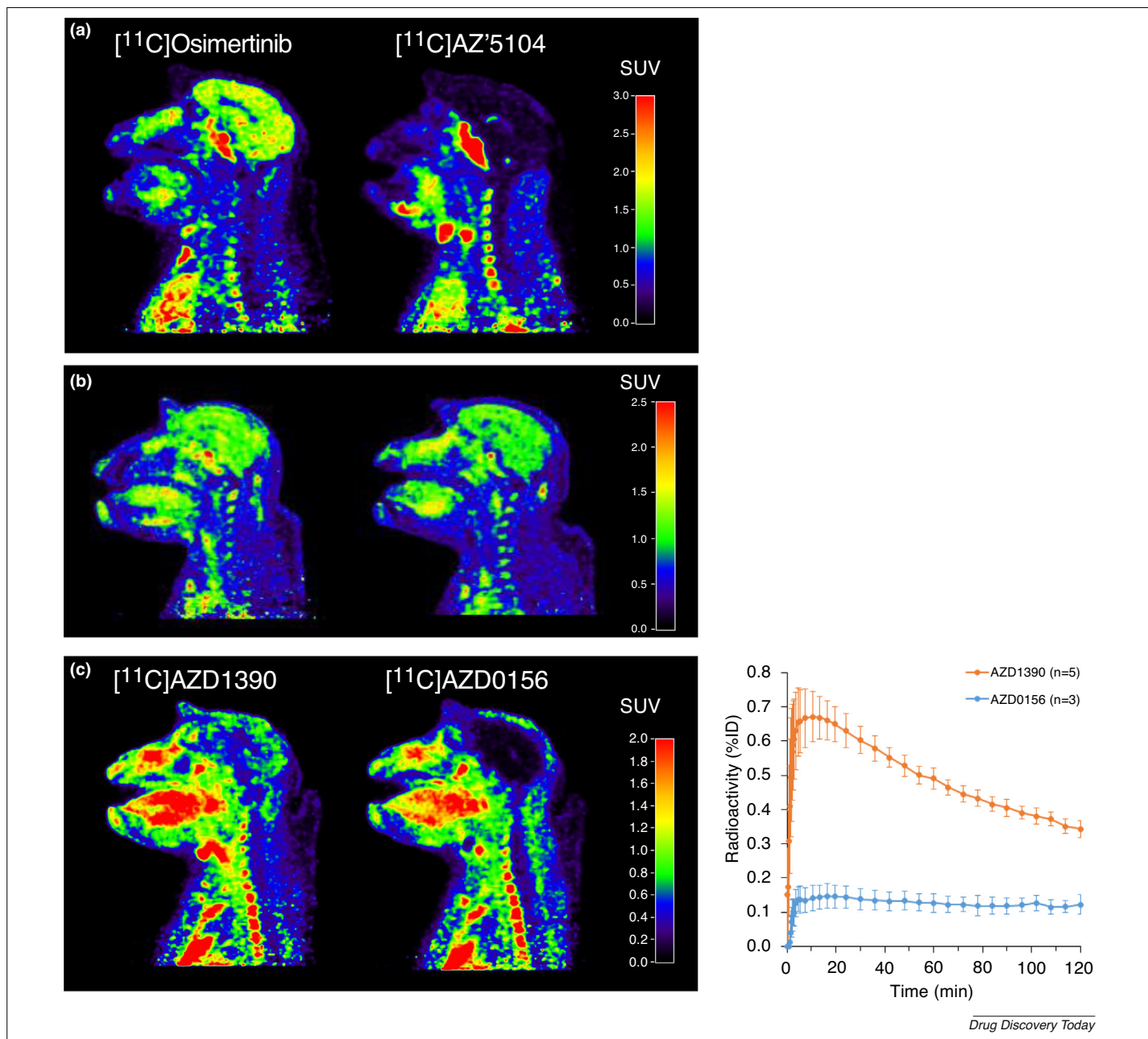


FIGURE 1

Color-coded PET images showing the distribution of radioactivity in the macaque brain following administration of microdoses of (a) [^{11}C]osimertinib and metabolite [^{11}C]AZ'5104 [21], (b) [^{11}C]AZD3759 [44], and (c) [^{11}C]AZD1390 and [^{11}C]AZD0156 [30]. The images represent average radioactivity from 5 to 123 min after injection. Image intensity is displayed as (SUV), corresponding to local radioactivity concentration normalized for injected radioactivity and body weight. In (c), both ataxia telangiectasia mutated (ATM) compounds were administered to the same monkey on the same day. Radioactivity versus time profiles represent averages across five and three independent macaque studies for AZ1390 and AZD0156, respectively [30]. Figure 1(c) ©The Authors, some rights reserved; exclusive licensee American Association for the Advancement of Science. Distributed under a Creative Commons Attribution Non Commercial Licence 4.0 (CC BY-NC) <http://creativecommons.org/licenses/by-nc/4.0/>.

recently at AZ, a double-transfected transporter MDCKII canine cell line, MDCK_MDR1_BCRP, has been developed containing overexpressed human MDR1 and human BCRP. This MDCK assay has the advantage of being able to rapidly assess compounds against both efflux transporters in one assay. This assay was utilized in the design and discovery of AZD1390 [30] and is

now routinely used as the primary BBB screen at AZ (Fig. 2).

***In vivo* rodent assessment**

In designing compounds with good brain exposure brain K_{pu} is a key parameter reflecting the concentration of free drug in the brain relative to the plasma at equilibrium. Ideally, a

$K_{pu} \geq 1$ is desirable, indicating a fully BBB-penetrant compound ($K_{pu} = 1$ indicating a purely passively permeable compound and $K_{pu} > 1$ supporting involvement of active uptake transporters). In practical terms, in drug discovery, a K_{pu} target > 0.3 is often used, whereas poorly BBB-penetrant compounds have K_{pu} values < 0.05 .

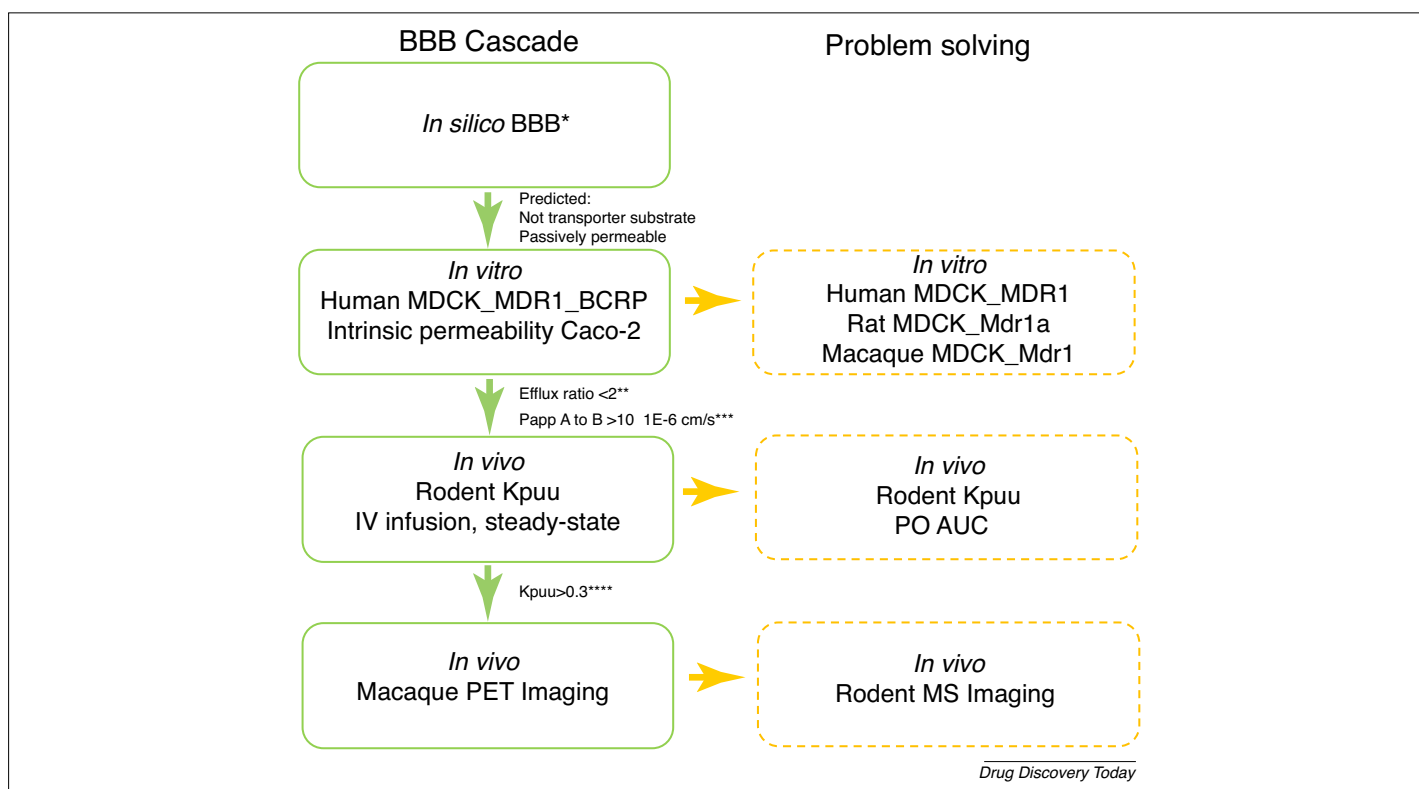


FIGURE 2

Identifying oncology drugs with good brain exposure – profiling cascade with target criteria. **In silico* models used include global and local models for transporter efflux, intrinsic permeability, and free brain:free plasma ratios (Kpuu) [33,34,35] to prioritize compounds for synthesis. **Intrinsically permeable compounds giving borderline efflux ratios ≥ 2 can be progressed to rodent Kpuu studies particularly if moderate human brain Kpuu values (0.3–0.05) are acceptable in the clinic because of a projected sizable safety margin. ***Intrinsic (in the presence of efflux inhibitors) Caco-2 A to B Papp at pH7.4/7.4 of $>10^{-6}$ cm/s represents high passive permeability (diffusion rate limited) in our laboratory. This value might differ across laboratories and so requires calibration. ****Compounds with moderate rodent Kpuu can be progressed into monkey PET if species differences identified from *in vitro* experiments or moderate Kpuu values are acceptable in the clinic. A predicted human Kpuu range can be derived from a consideration of the weight of evidence from human *in vitro* assays together with both rodent and monkey Kpuu values, taking into account any species differences that emerge at an *in vitro* and *in vivo* level. Abbreviations: AUC, area under the curve; BBB, blood–brain barrier; MDCK, Madin–Darby canine kidney; MS, mass spectroscopy.

The rat brain Kpuu represents a useful model for human brain Kpuu. Figure 3 shows the rat brain Kpuu values for a range of marketed drugs [33], highlighting the typically higher Kpuu values achieved by CNS drugs. The P-gp transporter levels, as measured by protein expression, in the rat BBB are threefold higher than in humans [25]. P-gp is the most highly expressed transporter in the rat BBB, fourfold higher than the levels of rat BCRP [25]. By contrast, BCRP is the most highly expressed transporter in the human BBB, at 8.14 fmol/mg protein compared with the P-gp transporter at 6.06 fmol/mg protein [25]. Differences in species expression levels mean that, for purely P-gp substrates, rodent Kpuu values tend to be lower than those of primates and humans [26,36]. The amino acid sequence homology with the human P-gp transporter is reported as 85% for rat (mouse is 87%) [26]. As such, there are typically few species differences between rodents and humans in terms of efflux transporter substrate specificity, although exceptions do arise [26,37] and, as

such, rat and macaque mdr1 assays are available to assess any species difference potential at the *in vitro* level.

Rat brain Kpuu values are determined from *in vivo* measurement of Kp combined with the *in vitro*-determined fraction unbound in brain (fub) and fraction unbound in plasma (fup): that is, $Kpuu = Kp \times fub/fup$. At AZ, rodent brain Kp values are determined by two main methods: (i) IV steady-state infusion; and (ii) area under the curve (AUC) based (Fig. 2). The infusion assay utilizes a 4-h constant infusion of a cassette of three compounds dosed to three rats. Steady state is assumed to have been reached at 4 h when brain and plasma samples are collected ($Kp = \text{brain/plasma at 4 h}$). The AUC-based method typically involves an oral dose to six rats, sampling brain and plasma across a time course from 0 to 16 h ($Kp = \text{AUC}_{\text{brain}}/\text{AUC}_{\text{plasma}}$). The infusion method offers the advantage of utilizing fewer animals per compound than the other method and is a useful approach where poor exposure by other dosing routes limits compound detection.

As such, it is used as the primary *in vivo* assay at AZ (Fig. 2). The AUC-based method offers the advantage of being able to observe whether the brain and plasma profiles are parallel, indicating that equilibration has been rapidly achieved. The profiles also enable an early indication of the duration of brain exposure relative to potency measures [30].

In determining Kpuu, it is advantageous to use a rat brain slice-binding fub rather than fub from a homogenate method [38]. The rat brain slices retain their cellular integrity, ensuring physiological mechanisms such as nonspecific and specific binding, pH partitioning across intracellular lysosomes, and active transport mechanisms, are retained. This is particularly important for bases where lysosomal trapping can be missed in the homogenate method and give rise to artifactually elevated Kpuu values.

Brain imaging

PET microdosing allows the distribution of compounds in the healthy brain of primates to

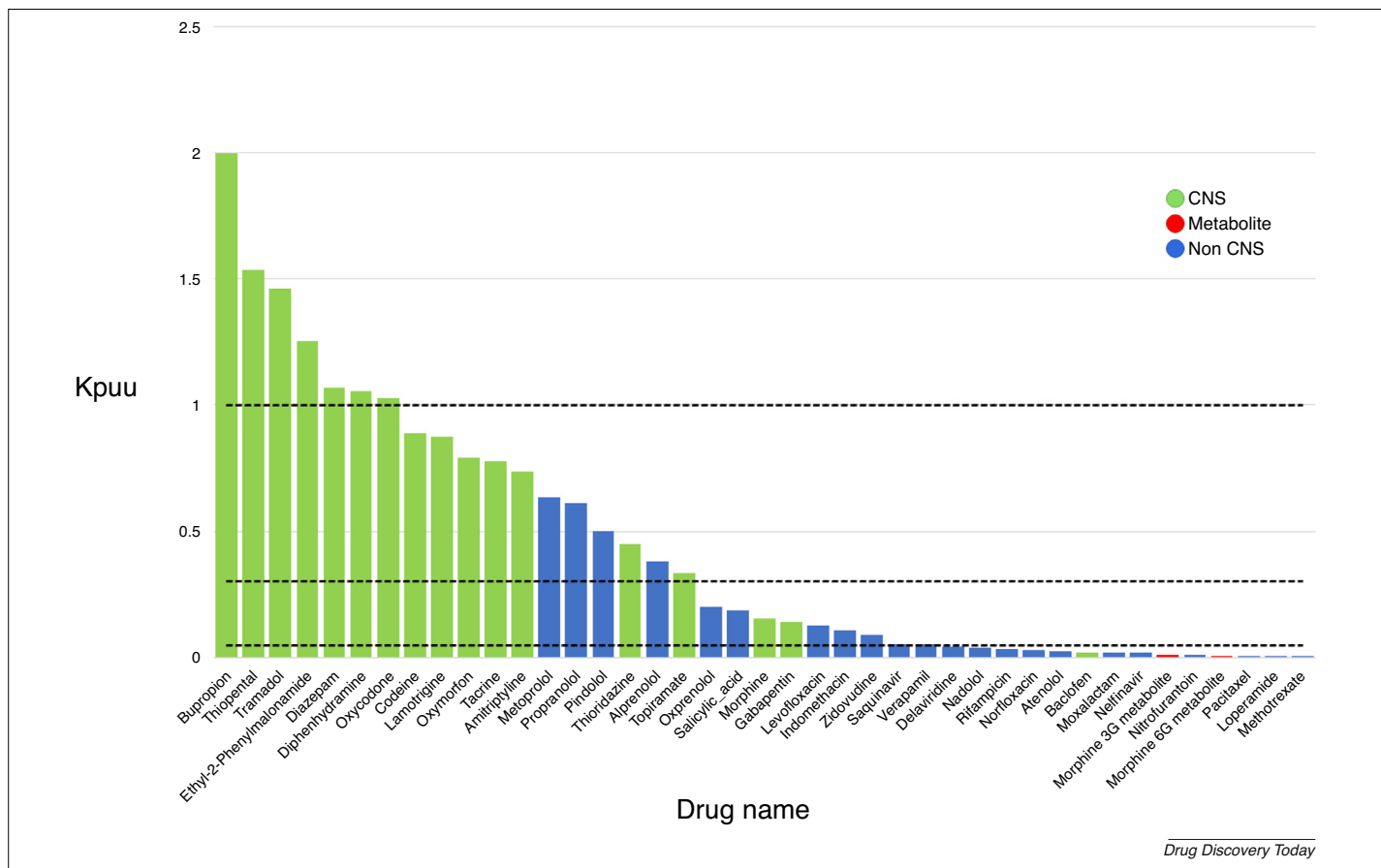


FIGURE 3

Rat brain Kp_u values for a range of marketed drugs. Horizontal lines reflect Kp_u 1, 0.3, and 0.05. Kp_u values calculated from rat Kp (intravenous steady-state infusion method), fub (rat brain slice-binding method), and fup (rat plasma binding by equilibrium dialysis). Data from Ref. [33].

be studied (Fig. 1a–c) [27]. This is particularly important for discovery projects since primates represent the closest brain model to humans [25,26], with *in vivo* studies to date supporting good concordance between the species [36,39]. At AZ, access to an *in vitro* efflux assay using an MDCK cell line transfected with the macaque P-gp transporter (Fig. 2) is facilitating knowledge around species difference to be further evaluated. In addition to imaging, quantitative measures of brain penetration, including the percentage of injected radioactivity at C_{max} (% ID or normalized to injected dose and body weight, SUV), Kp, and Kp_u can be derived from PET studies. Kp values are most accurately determined using one or two compartmental models [27]. For reversible binding compounds, this can be combined with rat brain-binding fub (which is species independent [40]) and macaque plasma-binding data to generate Kp_u (e.g., as detailed for AZD1390, which determined a Kp_u of 0.33 [30]). In a macaque PET study looking at 12 CNS drugs, Schou *et al.* showed that ten CNS drugs had Kp_u values ≥ 0.3 [27].

This is consistent with the rat Kp_u analysis in Fig. 3, which also showed that most CNS drugs have Kp_u >0.3.

Mass spectroscopy imaging (MSI) is a powerful tool enabling the distribution of unlabeled compound and/or metabolites to be simultaneously assessed in healthy brain tissue and in intracranial tumors in preclinical species. It is a developing area offering the opportunity to further increase confidence and understanding of the ability of discovery molecules to penetrate the BBB [41]. In healthy brain tissue, MSI allows compounds restricted to the vasculature by the BBB to be identified and the effects of efflux transporters on poor penetration to be understood [42,43].

Case example: AZD3759

AZD3759 is a reversible first-generation oral EGFR-TKI inhibitor sensitive to the activating mutations of EGFR [29,44]. It is the first EGFR-TKI designed to cross the BBB to treat NSCLC EGFRm with CNS metastases [44]. Data from the BLOOM Phase I clinical trial in patients with advanced EGFRm NSCLC not previously treated with EGFR

TKIs showed CNS activity for AZD3759 [45]. In these patients, AZD3759 at 200 or 300 mg twice daily resulted in a confirmed objective response rate of 83% in CNS lesions and 72% in extracranial lesions. A Kp_{u,CSF} of 1.11 (free CSF/free plasma ratio) was also determined, reflecting the absence of efflux substrate activity.

In developing AZD3759, gefitinib was used as the lead for the project with the goal to design in good brain penetration properties [44]. Although very challenging, this was achieved by removing transporter efflux liability. This included approaches such as masking hydrogen bond-donating effects through introduction of intramolecular hydrogen bonding [44]. AZD3759 was identified as not being a substrate for human efflux transporters and, therefore, having good BBB penetration by utilizing *in vitro* MDCK studies with cell lines transfected with human P-gp or BCRP and also rat and mouse *in vivo* studies where equilibrium free brain and free blood levels are essentially equivalent (Kp_u = 1.3 and 0.65, respectively) [44]. PET imaging studies in macaques also showed that

AZD3759 readily distributes throughout the brain (Fig. 1b), with $K_{puu} = 0.5$ and 0.53 [44].

Case example: AZD1390

AZD1390 is a highly potent inhibitor of ataxia telangiectasia mutated (ATM) kinase, designed to cross the BBB and which causes radiosensitization of GBM cells [30]. It is currently in clinical development for the treatment of GBM in combination with radiotherapy.

AZ previously developed the potent and selective ATM inhibitor AZD0156 for the treatment of systemic tumors [46]. AZD0156 is a substrate for human efflux transporters (efflux ratio = 23 in the MDCK_MDR1_BCRP assay) and, therefore, unlikely to significantly cross the BBB [30]. In designing AZD1390, the challenge was to optimize further to generate an ATM inhibitor with good BBB penetration for GBM. As such, the discovery team sort to design compounds without human efflux transporter liability using *in vitro* MDCK efflux transporter assays [30].

AZD1390 was identified as having significant BBB penetration with an absence of human transporter efflux observed in the MDCK_MDR1_BCRP and MDCK_MDR1 assays (efflux ratio <2). AZD1390 appears to be a weak substrate for rodent transporters, as seen in *in vitro* and *in vivo* inhibitor studies with a moderate rat brain K_{puu} of 0.17. Good free levels of AZD1390 are achieved in the brain (above IC_{50}) at tolerated doses in mice and demonstrate a significant increase in animal survival in an orthotopic GBM model (GL261) [30]. Macaque PET images (Fig. 1c) demonstrate that AZD1390 gives significant brain penetration with a C_{max} (%ID) of 0.68 ± 0.078 ($N = 5$) and K_{puu} 0.33. In contrast AZD0156 shows poor brain penetration [C_{max} (%ID) 0.15 ± 0.036 ($N = 3$)]. (K_p could not be derived from the PET data of AZD0156 because of high standard errors in the data fitting and, therefore, K_{puu} was not reported.)

Concluding remarks

Designing molecules to remove efflux transporter liability is key to achieving high brain K_{puu} . In practical terms, discovery projects require a K_{puu} value that delivers unbound drug levels in the brain for the necessary duration to drive clinical efficacy. To address the high unmet need of oncology patients with primary and secondary brain malignancies, future therapeutic agents will be required to cross the BBB and achieve good brain exposure at tolerated doses. Although challenging to design such molecules, the availability of new *in vitro* human transporter assays, K_{puu} rodent assays, and state-of-the-art imaging techniques ensures that a complementary range

of BBB tools can be exploited to rapidly identify brain-penetrant drugs.

Acknowledgments

We thank colleagues who contributed to the development of the AZ CNS strategy, including R. Alluri, M. Antonsson, S. Bagal, G. Brolén, R. Goodwin, I. Gurrell, A. Fretland, A. Janefeldt, P. Nordell, A. Pike, V. Pilla Reddy, A. Sykes and S. Winiwarer. We also thank members of the PET group at the Karolinska Institutet for technical support. Human MDR1-transfected MDCK cells (MDCK_MDR1) were obtained from the Netherland Cancer Institute (NKI-AVL). This cell line was transfected with human BCRP internally (Asia IMED, IMED Biotech unit, AstraZeneca, Shanghai, China).

Conflicts of interest

The following authors hold stock in AZ: N.C., P.J., and D.M.

References

- Rangachari, D. *et al.* (2015) Brain metastases in patients with EGFR-mutated or ALK-rearranged non-small-cell lung cancers. *Lung Cancer* 88, 108–111
- Yamanaka, R. (2009) Medical management of brain metastases from lung cancer. *Oncol. Rep.* 22, 1269–1276
- Ajaz, M. *et al.* (2014) Current and investigational drug strategies for glioblastoma. *Clin. Oncol.* 26, 419–430
- Delgado-López, P.D. and Corrales-García, E.M. (2016) Survival in glioblastoma: a review on the impact of treatment modalities. *Clin. Transl. Oncol.* 18, 1062–1071
- Stupp, R. *et al.* (2005) Radiotherapy plus concomitant and adjuvant temozolomide for glioblastoma. *N. Engl. J. Med.* 352, 987–996
- Lagerwaard, F.J. *et al.* (1999) Identification of prognostic factors in patients with brain metastases: a review of 1292 patients. *Int. J. Radiat. Oncol. Biol. Phys.* 43, 795–803
- Bohn, J. *et al.* (2016) Targeted therapies for the treatment of brain metastases in solid tumours. *Target Oncol.* 11, 263–275
- Urquhart, B.L. and Kim, R.B. (2009) Blood brain barrier (BBB) transporters and response to CNS-active drugs. *Eur. J. Clin. Pharmacol.* 65, 1063–1070
- Ha, S.N. *et al.* (2007) Mini review on molecular modeling of P-glycoprotein (P-gp). *Curr. Topics Med. Chem.* 7, 1525–1529
- Deeken, J.F. and Loscher, W. (2007) The blood–brain barrier and cancer: transporters, treatment and trojan horses. *Clin. Cancer Res.* 13, 1663–1674
- Zhang, R. *et al.* (1992) Differential permeability of the blood–brain barrier in experimental brain metastases produced by human neoplasms implanted into nude mice. *Am. J. Pathol.* 141, 1115–1124
- Van Tellingen, O. *et al.* (2015) Overcoming the blood–brain tumor barrier for effective glioblastoma treatment. *Drug Resist. Updates* 19, 1–12
- Oberoi, R.K. (2016) Strategies to improve delivery of anticancer drugs across the blood–brain barrier to treat glioblastoma. *NeuroOncology* 18, 27–36
- Fushiki, H. *et al.* (2016) Preclinical pharmacokinetic and pharmacological properties of ASP8273, a mutant-selective irreversible EGFR inhibitor, and its potential activity against brain metastases in NSCLC. *Eur. J. Cancer* 69 (Suppl. 1), S41
- Tonra, J.R. (2015) Blood brain barrier penetrant HER2/neu, Src, and EGFR inhibitor. *Cancer Res.* 75, 2590
- Finlay, M.R.V. *et al.* (2014) Discovery of a potent and selective EGFR Inhibitor (AZD9291) of both sensitizing and T790 M resistance mutations that spares the wild type form of the receptor. *J. Med. Chem.* 57, 8249–8267
- Cross, D.A. *et al.* (2014) AZD9291, an irreversible EGFR TKI, overcomes T790M-Mediated resistance to EGFR inhibitors in lung cancer. *Cancer Discov.* 4, 1046–1061
- Reungwetwattana, T. *et al.* (2018) CNS response to osimertinib versus standard epidermal growth factor receptor tyrosine kinase inhibitors in patients with untreated EGFR-mutated advanced non-small-cell lung cancer. *J. Clin. Oncol.* 36, 3290–3297
- Soria, J.C. *et al.* (2018) Osimertinib in untreated EGFR-mutated advanced non-small-cell lung cancer. *N. Engl. J. Med.* 378, 113–125
- Wu, Y. *et al.* (2018) CNS efficacy of osimertinib in patients with T790M-positive advanced non-small-cell lung cancer: data from a randomized Phase III trial (AURA3). *J. Clin. Oncol.* 36, 2702–2709
- Ballard, P. *et al.* (2016) Preclinical comparison of osimertinib with other EGFR-TKIs in EGFR-mutant NSCLC brain metastases models, and early evidence of clinical brain metastases activity. *Clin. Cancer Res.* 22, 1–11
- Owen, S. and Souhami, L. (2014) The management of brain metastases in non-small cell lung cancer. *Front. Oncol.* 4, 1–6
- DeVries, N.A. *et al.* (2012) Restricted brain penetration of the tyrosine kinase inhibitor erlotinib due to the drug transporters P-gp and BCRP. *Invest. New Drugs* 30, 443–449
- Yang, J.C.-H. *et al.* (2017) Osimertinib for patients (pts) with leptomeningeal metastases (LM) from EGFR-mutant non-small cell lung cancer (NSCLC): updated results from the BLOOM study. *J. Clin. Oncol.* 35 abstr 2020
- Nicolas, J.M. (2015) Species differences and impact of disease state on BBB. In *Blood–Brain Barrier in Drug Discovery* (Di, L. and Kerns, E.H., eds), pp. 66–93, Wiley
- Syvänen, S. *et al.* (2009) Species differences in blood–brain barrier transport of three positron emission tomography radioligands with emphasis on p-glycoprotein transport. *Drug Metab. Dispos.* 37, 635–643
- Schou, M. *et al.* (2015) Large variation in brain exposure of reference CNS drugs: a PET study in nonhuman primates. *Int. J. Neuropsychopharmacol.* 18 pyv036
- Kodama, R. *et al.* (2010) Age-related lesions in the cerebrum in middle-aged female cynomolgus monkeys. *Toxicol. Pathol.* 38, 303–311
- Yang, Z. *et al.* (2016) AZD3759, a BBB-penetrating EGFR inhibitor for the treatment of EGFR mutant NSCLC with CNS metastases. *Sci. Transl. Med.* 8 368ra172
- Durant, S.T. (2018) The brain-penetrant clinical ATM inhibitor AZD1390 radiosensitizes and improves survival of preclinical brain tumour models. *Sci. Adv.* 4 eaat1719
- Mahar Doan, K.M. *et al.* (2002) Passive permeability and P-glycoprotein-mediated efflux differentiate central nervous system (CNS) and non-CNS marketed drugs. *J. Pharm. Exp. Ther.* 303, 1029–1037
- Wager, T.T. (2010) Moving beyond rules: the development of a central nervous system multiparameter optimization (CNS MPO) approach to enable alignment of druglike properties. *ACS Chem. Neurosci.* 1, 435–449
- Fridén, M. *et al.* (2009) Structure-brain exposure relationships in rat and human using a novel data set of unbound drug concentrations in brain interstitial and cerebrospinal fluids. *J. Med. Chem.* 52, 6233–6243

- 34 Varadharajan, S. (2015) Exploring *in silico* prediction of the unbound brain-to-plasma drug concentration ratio: model validation, renewal, and interpretation. *J. Pharm. Sci.* 104, 1197–1206
- 35 Fredlund, L. *et al.* (2017) *In vitro* intrinsic permeability: a transporter-independent measure of Caco-2 cell permeability in drug design and development. *Mol. Pharm.* 14, 1601–1609
- 36 Feng, B. *et al.* (2018) Prediction of human brain penetration of P-glycoprotein and breast cancer resistance protein substrates using *in vitro* transporter studies and animal models. *J. Pharm. Sci.* 107, 2225–2235
- 37 Feng, B. *et al.* (2008) *In vitro* P-glycoprotein assays to predict the *in vivo* interactions of P-glycoprotein with drugs in the central nervous system. *Drug Metab. Dispos.* 36, 268–275
- 38 Fridén, M. *et al.* (2011) Measurement of unbound drug exposure in brain: modelling of pH partitioning explains diverging results between the brain slice and brain homogenate methods. *Drug Metab. Dispos.* 39, 353–362
- 39 Pierson, M.E. *et al.* (2008) [¹¹C]AZ10419369: A selective 5-HT_{1B} receptor radioligand suitable for positron emission tomography (PET). Characterization in the primate brain. *NeuroImage* 41, 1075–1085
- 40 Di, L. *et al.* (2011) Species independence in brain tissue binding using brain homogenates. *Drug Metab. Dispos.* 39, 1270–1277
- 41 Goodwin, R.J.A. *et al.* (2017) Mass spectrometry imaging in oncology drug discovery. *Adv. Cancer Res.* 134, 133–171
- 42 Swales, J.G. (2015) Mapping drug distribution in brain tissue using liquid extraction surface analysis mass spectrometry imaging. *Anal. Chem.* 87, 10146–10152
- 43 Vallianatou, T. *et al.* (2018) A mass spectrometry imaging approach for investigating how drug–drug interactions influence drug blood–brain barrier permeability. *NeuroImage* 172, 808–816
- 44 Zeng, Q. *et al.* (2015) Discovery and evaluation of clinical candidate AZD3759, a potent, oral active, central nervous system-penetrant, epidermal growth factor receptor tyrosine kinase inhibitor. *J. Med. Chem.* 58, 8200–8215
- 45 Ahn, M. *et al.* (2017) Activity and safety of AZD3759 in EGFR-mutant non-small-cell lung cancer with CNS metastases (BLOOM): a phase 1, open-label, dose-escalation and dose-expansion study. *Lancet Respir. Med.* 5, 891–902
- 46 Pike, K.G. (2018) The identification of potent, selective, and orally available inhibitors of ataxia telangiectasia mutated (ATM) kinase: the discovery of AZD0156 (8-[6-[3-(dimethylamino)propoxy]pyridin-3-yl]-3-methyl-1-(tetrahydro-2H-pyran-4-yl)-1,3-dihydro-2H-imidazo[4,5-c]quinolin-2-one). *J. Med. Chem.* 61, 3823–3841

Nicola Colclough^{1,*}

Kan Chen²

Peter Johnström³

Markus Fridén^{4,5}

Dermot F. McGinness¹

¹DMPK, Oncology, IMED Biotech Unit, AstraZeneca, Cambridge, UK

²DMPK, Asia IMED, IMED Biotech Unit, AstraZeneca, Shanghai, China

³PET Science Centre, Precision Medicine and Genomics, IMED Biotech Unit, AstraZeneca, Karolinska Institutet, Stockholm, Sweden

⁴DMPK, RIA, IMED Biotech Unit, AstraZeneca, Gothenburg, Sweden

⁵Translational PKPD, Department of Pharmaceutical Biosciences, Uppsala University, Uppsala, Sweden

*Corresponding author.